

PAPER • OPEN ACCESS

## Modelling of sprays: simple solutions of complex problems

To cite this article: S Sazhin *et al* 2019 *J. Phys.: Conf. Ser.* **1368** 042059

View the [article online](#) for updates and enhancements.



**IOP | ebooks™**

Bringing you innovative digital publishing with leading voices to create your essential collection of books in STEM research.

Start exploring the **collection** - download the first chapter of every title for free.

# Modelling of sprays: simple solutions of complex problems

**S Sazhin<sup>1</sup>, E Shchepakina<sup>2</sup> and V Sobolev<sup>2</sup>**

<sup>1</sup>Sir Harry Ricardo Laboratories, Advanced Engineering Centre, School of Computing, Engineering and Mathematics, University of Brighton, Brighton BN2 4GJ, UK

<sup>2</sup>Samara National Research University, 34, Moskovskoye Shosse, Samara 443086, Russia

e-mail: [S.Sazhin@brighton.ac.uk](mailto:S.Sazhin@brighton.ac.uk)

**Abstract.** Some new approaches to the solution of complex problems, focused on spray modelling, using relatively simple mathematical tools are briefly summarised. The following problems are considered: modelling of spray drying with pharmaceutical applications, modelling of heating and evaporation of suspended droplets with applications to water sprays for fire suppression, modelling of micro-explosions with automotive applications, and parameterisations of slow invariant manifolds with applications to spray ignition modelling. The modelling of spray drying is based on the assumption that the array of small suspended solid particles inside droplets can be treated as a non-evaporating liquid component. The modelling of the effect of a support rod on droplet heating and evaporation is based on the assumption that this heat is homogeneously distributed inside the whole volume of a droplet. In the modelling of a puffing/micro-explosion it is assumed that a water sub-droplet is located exactly at the centre of a fuel droplet and the temperature at the surface of the fuel droplet is fixed. In the presentation of slow invariant manifolds in parametric form these manifolds are found using asymptotic expansions.

## 1. Introduction

Modelling of sprays is known to be a very complex problem, including the hydrodynamic interaction of droplets between themselves and ambient gas, heating and evaporation of interacting droplets, and possible ignition and combustion of a fuel vapour/air mixture in the case of fuel sprays [1]. This makes simplification of the models unavoidable. This simplification, however, might lead to the modelling of structures which have little in common with realistic sprays observed and/or used in engineering, pharmaceutical and environmental applications. Thus, it is necessary to find a reasonable compromise that simplifies the model and produces accurate predictions. One of the ways to achieve this is to make sure that the accuracies of all sub-models on which the spray model is based are similar.

The results of the development of the models of spray formation/dynamics, droplet heating and evaporation, and ignition of fuel vapour air mixture, focused on ensuring a reasonable compromise between the simplicity of the models and their accuracy, have been summarised in [2, 3, 4, 5]. This paper is essentially complementary to the above-mentioned book and reviews and is focused on the most recent developments not described in [2, 3, 4, 5]. All results presented in this paper have been previously published in leading international refereed journals in this and related fields. These journals, however, are rather specialised and are not well known to the wider community of researchers involved in mathematical modelling. Hence, the rationale for preparing this review.



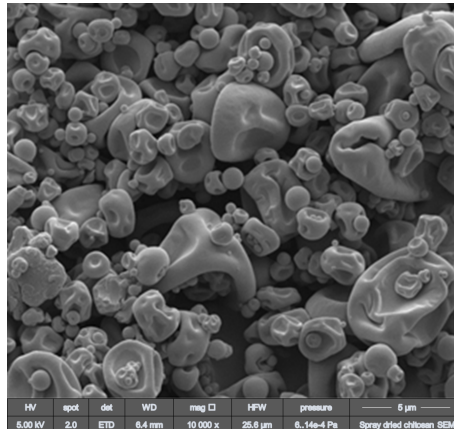


**Figure 1.** A typical micrograph for spray-dried chitosan particles. Reprinted from International Journal of Heat and Mass Transfer, Volume 122, Sazhin et al., A new model for a drying droplet, Pages 451-458, Copyright Elsevier (2018).

In Section 2 the results of the development of a new model for droplet drying are summarised. Section 3 is focused on the analysis of our new approach to taking into account the effects of support on heating and evaporation of water droplets. A simplified model for micro-explosions of fuel droplets with water sub-droplets in them is presented and discussed in Section 4. Section 5 is focused on the new approaches to parameterisations of slow invariant manifolds.

## 2. Modelling of droplet drying

The importance of modelling droplet drying in various pharmaceutical and engineering applications has been discussed in many papers including [6, 7, 8, 9]. Several models for this process have been suggested [9]. A number of simplifying assumptions have been used in these models, including ignoring the temperature gradient inside droplets, the applicability of which is not at first obvious. In contrast to previously suggested models, the model described in [10] not only takes into account most effects ignored in the previous models but also appears to be much simpler than those suggested earlier. The main ideas of this model are described below, following [10].

In the model described in [10], small solid particles in an ambient evaporating liquid, or a non-evaporating substance in this liquid, are considered as a non-evaporating liquid component. Analytical solutions to the species diffusion and heat transfer equations inside droplets in this model are used at each time step. These solutions are exactly the same as described in [2], but

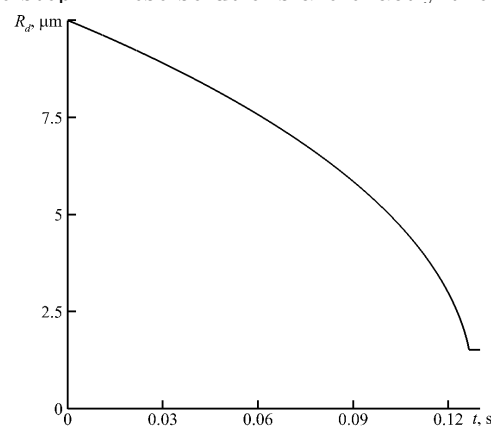


**Figure 2.** Droplet radius versus time for input parameters described in the text of the paper. Reprinted from International Journal of Heat and Mass Transfer, Volume 122, Sazhin et al., A new model for a drying droplet, Pages 451-458, Copyright Elsevier (2018).

for the boundary conditions it was assumed that the relative mass fraction of solid particles in the vapour phase is zero. Partial pressure of vapour at the droplet's surface was estimated from Raoult's law.

The model was developed to describe the process of spray drying leading to the production of chitosan particles, shown in Figure 1. The following input parameters were used for numerical simulations based on the above-mentioned model. The density of chitosan was assumed equal to  $1300 \text{ kg/m}^3$  (similar to cellulose acetate) and not dependent on temperature. Also, the density of water was assumed constant and equal to  $945.2 \text{ kg/m}^3$ . The specific heat capacity of chitosan was taken equal to  $1.6747 \text{ kJ/(kg K)}$ . Data presented in [11] were used to estimate the specific heat capacity of water. Droplets were prepared from a solution of  $0.2 \text{ g}$  polymer in  $50 \text{ g}$  water [12]. Thus the initial mass fractions of the polymer and water in the droplets were  $0.004$  and  $0.996$ , respectively.

The plot of the time evolution of the droplet radius is shown in Figure 2. As one can see from this figure, the droplet evaporation process can be seen until approximately  $t = 0.127 \text{ s}$ . Then, the evaporation stops and the droplet becomes a solid polymer ball with radius  $1.51 \mu\text{m}$ . This radius is approximately 6% larger than the one inferred from the initial mass of chitosan. The reason for this is not fully understood. Note that the problems associated with accurate calculation of droplet radii at the final stages of droplet evaporation are well known [2].

### 3. Modelling of suspended droplets

In most experiments focused on investigation of droplet heating and evaporation processes, including those performed for optimising water spray fire extinguishers, the droplets under consideration are suspended on a supporting rod (support) rather than free moving. An example of such a suspended droplet, taken from [13], is shown in Figure 3.

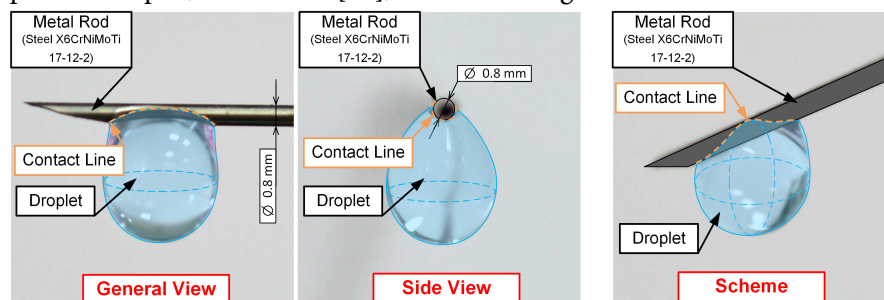


**Figure 3.** A general view and schematics of a droplet supported by a hollow metal rod. Reprinted from International Journal of Heat and Mass Transfer, Volume 127, Stryzhak et al., Heating and evaporation of suspended water droplets: Experimental studies and modelling, Pages 92-106, Copyright Elsevier (2018).

The presence of a suspension rod makes the problem of modelling droplet heating and evaporation much more complex compared with the case of free moving droplets as in this case we cannot assume that the problem is spherically symmetric (as for droplets suspended in microgravity conditions) and cannot use the Effective Thermal Conductivity/Effective Diffusivity models as in the case of moving droplets [2]. The traditional approach in such circumstances is based on the application of 2D or even 3D models (e.g. [14]). The problem with using this approach to modelling lies not only in its complexity, but also in the fact that this complexity does not lead to improved accuracy and reliability of the model in the general case. For example in these models it is typically assumed that the droplets are spherical and the area of contact between the droplet and the support can be accurately determined. The accuracy of these assumptions is far from obvious and they typically introduce uncontrollable errors into the model predictions despite the complexity of the model.

The main idea behind the model suggested in [13] is to reduce the 3D problem of modelling the effect of support on droplet heating and evaporation to a 1D problem with minimal loss of accuracy in the model predictions.

The new model for droplet heating in the presence of a support is based on the assumption that droplets are spherical and their surfaces are heated by convection, while the effect of the support is described using a heating source term, similar to that describing the effect of thermal radiation. This source term is assumed to be spherically symmetric; the error introduced by this assumption is expected to be comparable to that caused by the assumption that the droplet is spherical. The effect of gas motion around the droplet is described in terms of the Effective Thermal Conductivity model [2].

These assumptions allow us to write the equation for temperature inside droplets ( $T$ ) as

$$\frac{\partial T}{\partial t} = \kappa \left( \frac{\partial^2 T}{\partial R^2} + \frac{2}{R} \frac{\partial T}{\partial R} \right) + P(R), \quad (1)$$

where

$$\kappa = k_{\text{eff}} / (c_l \rho_l) \quad (2)$$

is the effective thermal diffusivity,  $c_l$  is specific liquid heat capacity,  $\rho_l$  is liquid density,  $R$  is the distance from the centre of the droplet,  $t$  is time, and the source term  $P(R)$  takes into account the effects of the supporting rod to be discussed later (in the models described in [2] this term took into account droplet heating by external thermal radiation).

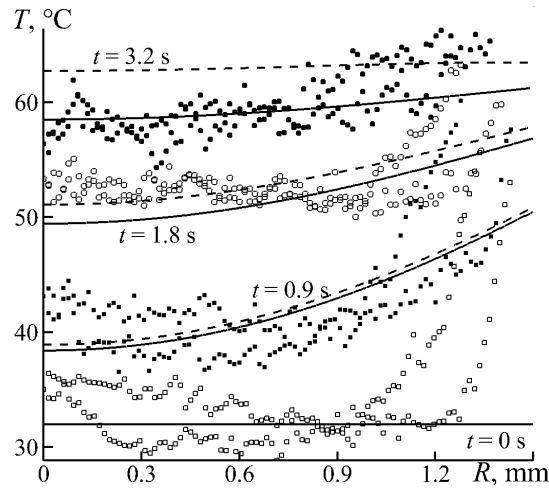


**Figure 4.** Temperatures inside the droplets versus the distance from the droplet centre at four time instants and ambient gas temperature 500°C; the droplet initial radius is  $R_d = 1.53$  mm. Reprinted from International Journal of Heat and Mass Transfer, Volume 127, Stryzhak et al., Heating and evaporation of suspended water droplets: Experimental studies and modelling, Pages 92-106, Copyright Elsevier (2018).

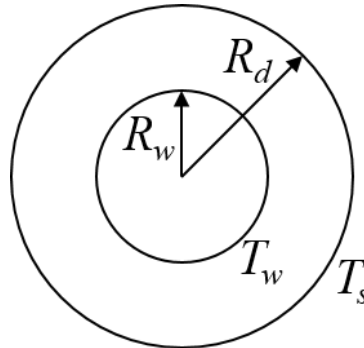


**Figure 5.** The location of a water sub-droplet of radius  $R_w$  inside a fuel droplet of radius  $R_d$ .  $T_w$  and  $T_s$  are the temperatures at the interface between water and fuel and at the droplet surface, respectively. Reprinted from International Journal of Heat and Mass Transfer, Volume 131, Sazhin et al., A simple model for puffing/micro-explosions in water-fuel emulsion droplets, Pages 815-821, Copyright Elsevier (2019).

This equation was solved subject to the standard initial and Robin boundary conditions [2], assuming that the convection heat transfer coefficient  $h$  is constant [2]:

$$T(R, t) = \frac{R_d}{R} \sum_{n=1}^{\infty} \left\{ \frac{p_n}{\kappa_R \lambda_n^2} + \exp \left[ -\kappa_R \lambda_n^2 t \right] \left( q_n - \frac{p_n}{\kappa_R \lambda_n^2} \right) - \frac{\sin \lambda_n}{\|v_n\|^2 \lambda_n^2} \mu_0(0) \exp \left[ -\kappa_R \lambda_n^2 t \right] \right. \\ \left. - \frac{\sin \lambda_n}{\|v_n\|^2 \lambda_n^2} \int_0^t \frac{d\mu_0(\tau)}{d\tau} \exp \left[ -\kappa_R \lambda_n^2 (t - \tau) \right] d\tau \right\} \sin \left[ \lambda_n \left( \frac{R}{R_d} \right) \right] + T_a(t), \quad (3)$$

where:

$$p_n = \frac{1}{R_d^2 \|v_n\|^2} \int_0^{R_d} (RP(R)) \sin(\lambda_n R/R_d) dR,$$

$\lambda_n$  are solutions to the equation:

$$\lambda \cos \lambda + h_0 \sin \lambda = 0, \quad (4)$$

$$\|v_n\|^2 = \frac{1}{2} \left( 1 - \frac{\sin 2\lambda_n}{2\lambda_n} \right) = \frac{1}{2} \left( 1 + \frac{h_0}{h_0^2 + \lambda_n^2} \right),$$

$$q_n = \frac{1}{R_d \|v_n\|^2} \int_0^{R_d} \tilde{T}_0(R) \sin \left[ \lambda_n \left( \frac{R}{R_d} \right) \right] dR, \quad \kappa_R = \frac{k_{\text{eff}}}{c_l \rho_l R_d^2}, \quad \mu_0(t) = \frac{h T_g(t) R_d}{k_{\text{eff}}},$$

$h_0 = (h R_d / k_{\text{eff}}) - 1$ ,  $\tilde{T}_0(R) = R T_{d0}(R) / R_d$ . The solution to Equation (4) gives a set of positive eigenvalues  $\lambda_n$  (numbered in ascending order,  $n = 1, 2, \dots$ ). The term proportional to  $\frac{d\mu_0(\tau)}{d\tau}$  in (3) is small; it was ignored in our calculations.

Solution (3) was applied to modelling droplet heating during a short time step  $\Delta t$ . The effect of evaporation in (3) was taken into account by replacing air temperature  $T_a$  with:

$$T_{\text{eff}} = T_a + \frac{\rho_l L \dot{R}_{de}}{h}, \quad (5)$$

where  $L$  is the latent heat of evaporation, and the value of the change in droplet radius due to evaporation  $\dot{R}_{de}$  was estimated from the droplet evaporation rate during the previous time step. The droplet radius  $R_d$  and the convection heat transfer coefficient  $h$  were assumed constant, but were updated at the end of the time step. The conventional Abramzon and Sirignano model (see [2]) was used to describe droplet evaporation. The effects of swelling were taken into account as in [2].

The rate of heat supplied via the support to the droplet was estimated as:

$$q = \frac{k_w (T_{\text{sup}} - T_c)}{R_d} S_c, \quad (6)$$

where  $k_w$  is the thermal conductivity of water (at the average droplet temperature),  $T_c$  is the temperature at the centre of the droplet,  $T_{\text{sup}}$  is the surface temperature of the support,  $S_c$  is an estimation of the contact area between the droplet and support (assumed to be constant). All input parameters in (6) were time dependent; this equation was applied during short time steps. The value of  $T_c$  was taken from the results of calculations based on Solution (3).

It was assumed that heat supplied to droplets through the support is homogeneously distributed throughout the droplet volume. Thus, heat supplied per unit droplet volume was estimated as:

$$q_v = \frac{3k_w (T_{\text{sup}} - T_c)}{4\pi R_d^4} S_c. \quad (7)$$

**Table 1.** Support temperatures (in °C) at four time instants and four gas temperatures taken from [13].

$t(\text{s})$	$T_a = 100^\circ\text{C}$	$T_a = 300^\circ\text{C}$	$T_a = 500^\circ\text{C}$	$T_a = 800^\circ\text{C}$
0	30	30	30	30
5	57	99	164	267
15	61	122	205	
30	63	138	229	

**Table 2.** The initial temperatures of droplets at four gas temperatures.

	$T_a = 100^\circ\text{C}$	$T_a = 300^\circ\text{C}$	$T_a = 500^\circ\text{C}$	$T_a = 800^\circ\text{C}$
$T_0$	$19^\circ\text{C}$	$25^\circ\text{C}$	$32^\circ\text{C}$	$39^\circ\text{C}$

This allows us to consider the additional effect of heating droplets via the support in terms of a source term in Equations (1) and (3) assuming that

$$P(R) = \frac{3k_w(T_{\text{sup}} - T_c)}{4\pi c_l \rho_l R_d^4} S_c. \quad (8)$$

This expression was used in (3) for prediction of the distribution of temperature inside the droplets as a function of time.

The time evolution of the temperature of the support in the experiments performed in [13] for four gas temperatures is presented in Table 1. The initial droplet temperatures at these gas temperatures are shown in Table 2.

The predicted and observed distributions of temperatures inside the droplets versus the distance from the droplet centre at four time instants (0 s, 4 s, 8 s and 12 s) are shown in Figure 4 for ambient gas temperature equal to  $500^\circ\text{C}$ . Symbols show experimental results obtained in two perpendicular directions; solid and dashed curves show model predictions assuming that ambient gas temperature is equal to  $400^\circ\text{C}$ , ignoring and taking into account the effect of the support, respectively. The reduced gas temperature used in the modelling took into account gas cooling during droplet heating and evaporation (this was a fitting parameter in our model).

In all cases the predicted droplet temperatures increase with time in agreement with experimental data. Also, the predicted increase in temperatures inside the droplets with increasing distance from the droplet centre is consistent with the results of experimental observations. Similar results were obtained for gas temperatures  $100^\circ\text{C}$ ,  $300^\circ\text{C}$  and  $800^\circ\text{C}$ .

#### 4. Modelling of micro-explosions

It is widely believed that fuel mixing and internal combustion engine efficiency can be improved if puffing and micro-explosion in fuel droplets containing water sub-droplets takes place [15]. These are able to promote the secondary atomization process via a rapid break-up of the parent droplets due to the difference in volatility of the fuel and water. Puffing is the partial ejection of the dispersed water vapour out of an emulsion droplet, while micro-explosion refers to the complete break-up of the parent droplet [16, 17, 18]. The roles of these phenomena in internal combustion engines have been widely discussed in the literature (see [19] for the details).

A number of models for puffing/micro-explosions, starting with simple ones [20, 21] and ending with the most advanced ones [16, 17, 18], have been suggested. Nobody questions the usefulness of the models described in [16, 17, 18] for understanding the physical processes which take place during puffing/micro-explosions. However, their usefulness for engineering applications is not obvious. Engineers working with puffing and micro-explosions in droplets are mainly interested in such characteristics as the delays in puffing/micro-explosion, rather than in the processes which take place inside the deforming/exploding droplet. This was addressed in a relatively simple model of these processes suggested in [19]. In what follows the main ideas of this model are briefly summarised.

In the model suggested in [19] a small spherical water sub-droplet was placed in the centre of a larger fuel (n-dodecane) droplet (see Figure 5). The droplet was stationary; penetration of heat from the surface to the interior of the droplet was described by a one-dimensional transient heat conduction equation. This equation was solved analytically inside this composite droplet with the Dirichlet boundary condition at its surface. If  $T_s$  was greater than the initial homogeneous temperature inside the droplet, then the temperature between the centre of the droplet and its surface increased. If  $T_s$  was greater than the boiling temperature of water,  $T_w$  was expected to reach this boiling temperature at a certain time instant. This instant was identified as the start of the puffing/micro-explosion process (time to puffing or micro-explosion delay time). The maximal value of  $T_s$  was taken equal to the boiling temperature of n-dodecane.

The time evolution of the temperature inside the composite droplet is described by the heat conduction equation in the form [19]:

$$\frac{\partial T}{\partial t} = \kappa \left( \frac{\partial^2 T}{\partial R^2} + \frac{2}{R} \frac{\partial T}{\partial R} \right) + P(t, R), \quad (9)$$

where

$$\kappa = \begin{cases} \kappa_w = k_w / (c_w \rho_w) & \text{when } R \leq R_w \\ \kappa_f = k_f / (c_f \rho_f) & \text{when } R_w < R \leq R_d, \end{cases} \quad (10)$$

$\kappa_{w(f)}$  is the water (fuel) thermal diffusivity,  $k_{w(f)}$  is the water (fuel) thermal conductivity,  $c_{w(f)}$  is the water (fuel) specific heat capacity,  $\rho_{w(f)}$  is the water (fuel) density; the meaning of other parameters is the same as in (1). The source term  $P(t, R)$  takes into account volumetric droplet heating (e.g. heating due to thermal radiation). This was taken into account in the solution but was not used in the analysis presented in [19].

Equation (9) was solved analytically subject to the initial condition, boundary conditions at the interface between water and fuel, and the Dirichlet boundary condition at the surface of the droplet:

$$T|_{t=0} = \begin{cases} T_{w0}(R) & \text{when } R \leq R_w \\ T_{f0}(R) & \text{when } R_w < R \leq R_d, \end{cases} \quad (11)$$

$$T|_{R=R_w^-} = T|_{R=R_w^+}, \quad k_w \frac{\partial T}{\partial R} \Big|_{R=R_w^-} = k_f \frac{\partial T}{\partial R} \Big|_{R=R_w^+}, \quad (12)$$

$$T(R_d) \equiv T_s. \quad (13)$$

The solution to this mathematical problem was obtained using the following additional assumptions:

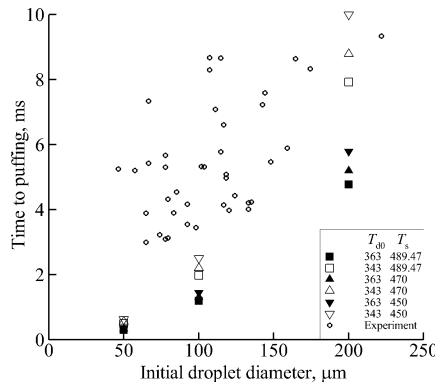


**Figure 6.** Time to puffing/micro-explosions, predicted by the model and inferred from experiments, versus the initial droplet diameters. Reprinted from International Journal of Heat and Mass Transfer, Volume 131, Sazhin et al., A simple model for puffing/micro-explosions in water-fuel emulsion droplets, Pages 815-821, Copyright Elsevier (2019).



1. The temperature of the droplet surface was constant during the whole period of its heating.
2. The effects of droplet evaporation and swelling can be ignored.
3. Both  $T_{w0}$  and  $T_{f0}$  did not depend on  $R$ .

**Table 3.** Droplet/gas initial conditions and properties.

Parameter	Value
Parent droplet radii ( $R_d$ ) [ $\mu\text{m}$ ]	25; 50; 100
Droplet initial composition [vol]	0.15 water + 0.85 n-dodecane
n-dodecane density ( $\rho_f$ ) [ $\text{kg}/\text{m}^3$ ]	825
Gas composition	air
Droplet surface temperatures ( $T_s$ ) [K]	489.47 (boiling temperature), 470, 450
Initial droplet temperature ( $T_{d0}$ ) [K]	343 and 363
Gas (air) pressure [MPa]	0.1

4. All thermodynamic and transport properties were taken at the initial droplet temperature.

These assumptions allowed the authors of [19] to derive the following analytical solution to Equation (9), subject to initial and boundary conditions (11), (12) and (13):

$$T(R, t) = T_s + \frac{1}{R} \sum_{n=1}^{\infty} \left[ \exp(-\lambda_n^2 t) (\Theta_{n1} + \Theta_{n2}) + \int_0^t \exp(-\lambda_n^2 (t - \tau)) p_n(\tau) d\tau \right] v_n(R), \quad (14)$$

where

$$\Theta_{n1} = \frac{T_0 c_w \rho_w}{||v_n||^2 (\lambda_n a_w)^2} [\lambda_n a_w R_w \cot(\lambda_n a_w R_w) - 1], \quad (15)$$

$$\Theta_{n2} = \frac{T_0 c_f \rho_f}{||v_n||^2 (\lambda_n a_f)^2} \left[ \lambda_n a_f R_w \cot(\lambda_n a_f (R_d - R_w)) - \frac{\lambda_n a_f R_d}{\sin(\lambda_n a_f (R_d - R_w))} + 1 \right], \quad (16)$$

$$T_0 = T_s - T_{w0} = T_s - T_{f0} \quad (17)$$

$$v_n(R) = \begin{cases} \pm \frac{\sin(\lambda_n a_w R)}{\sin(\lambda_n a_w R_w)} & \text{when } R < R_w \\ \pm \frac{\sin(\lambda_n a_f (R - R_d))}{\sin(\lambda_n a_f (R_w - R_d))} & \text{when } R_w \leq R \leq R_d, \end{cases} \quad (18)$$

$$||v_n||^2 = \frac{c_w \rho_w R_w}{2 \sin^2(\lambda_n a_w R_w)} + \frac{c_f \rho_f (R_d - R_w)}{2 \sin^2(\lambda_n a_f (R_w - R_d))} - \frac{k_w - k_f}{2 R_w \lambda_n^2},$$

$$p_n(t) = \frac{c_w \rho_w}{||v_n||^2} \int_0^{R_w} R P(t, R) v_n(R) dR.$$

A set of positive eigenvalues  $\lambda_n$  was found from the solution to the equation:

$$\sqrt{k_w c_w \rho_w} \cot(\lambda a_w R_w) - \sqrt{k_f c_f \rho_f} \cot(\lambda a_f (R_w - R_d)) = \frac{k_w - k_f}{R_w \lambda}, \quad (19)$$

$$0 < \lambda_1 < \lambda_2 < \dots \quad a_w = \sqrt{\frac{c_w \rho_w}{k_w}}, \quad a_f = \sqrt{\frac{c_f \rho_f}{k_f}}.$$

Sign ‘−’ was chosen in Expression (18) to obtain a physically meaningful solution when  $T \leq T_s$ . This solution was used for the analysis of puffing/micro-explosions observed during the experiments with the initial conditions shown in Table 3.

Using Solution (14), for all cases shown in Table 3, the values of time to puffing/micro-explosions were obtained [19]. These are shown in Figure 6 as functions of droplet diameters for various initial and surface droplet temperatures. In the same figure the experimentally observed times for various droplet diameters are shown.

As follows from Figure 6, the predicted times to puffing/micro-explosions for droplet surface temperature equal to the boiling temperature of n-dodecane are always less than those observed experimentally. In most cases, the orders of magnitude of the predicted and observed times for other values of droplet surface temperature are the same. The predicted increase in these times with the increase in the initial droplet diameters is consistent with experimental observations. The decrease in the surface temperature leads to an increase in this time, as expected. These results led the authors of [19] to conclude that the model which they suggested, despite its simplicity, is able to describe the processes leading to puffing/micro-explosions, not only qualitatively but also in some cases quantitatively.

## 5. Parameterisations of slow invariant manifolds

Some recent results, referring to slow invariant manifolds and their applications to modelling of sprays, originally published in [22], were discussed in our previous review [5]. In what follows, the new results referring to this topic, originally published in [23] and not included in [5], are briefly summarised.

In [23], some new effective techniques for investigation of singularly perturbed differential systems were described. These were based on the application of the invariant manifolds theory [24]. It was shown that the slow invariant manifold can sometimes be found in parametric form as a result of asymptotic expansions. If this was not possible, one needed to use an implicit presentation of the slow surface and obtain asymptotic representations for the slow invariant manifold in an implicit form. The results of the development of the mathematical theory of these approaches and the application of this theory to the analysis of the system of equations describing heating, evaporation, ignition and combustion of fuel sprays were presented. It was shown that the application of this new technique can allow one to reduce the number of equations describing these processes and eliminate the stiffness of the original system of equations.

## 6. References

- [1] Basu S, Agarwal A K, Mukhopadhyay A and C Patel C 2018 *Droplet and Spray. Application for Combustion and Propulsion* (Singapore: Springer)
- [2] Sazhin S S 2014 *Droplets and Sprays* (London: Springer)
- [3] Sazhin S S 2017 *Fuel* **196** 69
- [4] Sazhin S S 2018 *Droplet and Spray. Application for Combustion and Propulsion* (Singapore: Springer) **3** 7-76
- [5] Sazhin S S, Shchepakina E and Sobolev V A 2018 *J. Phys.: Conf. Series* **1096** 012052
- [6] Vehring R, Foss W R and Lechuga-Ballesteros D 2007 *J of Aerosol Science* **38** 728
- [7] Zhu Y-Y, Guo Y, Wang C-Y, Qiao Z-J and Chen M-M 2015 *Chemical Engineering Science* **135** 109
- [8] Singh A and Van den Mooter G 2016 *Advanced Drug Delivery Reviews* **100** 27
- [9] Porowska A, Dosta M, Fries L, Gianfrancesco A, Heinrich S and Palzer S 2016 *Chemical Engineering Research and Design* **110** 131
- [10] Sazhin S S, Rybdylova O, Pannala A S, Somavarapu S and Zaripov S K 2018 *International Journal of Heat and Mass Transfer* **122** 451
- [11] Yaws C L 2008 *Thermophysical Properties of Chemicals and Hydrocarbons* (William Andrew)
- [12] Merchant Z, Taylor K M G, Stapleton P, Razak S A, Kunda N, Alfagih I, Sheikh K, Saleem I Y and Somavarapu S 2014 *European Journal of Pharmaceutics and Biopharmaceutics* **88** 816
- [13] Strizhak P A, Volkov R S, Castanet G, Lemoine F, Rybdylova O and Sazhin S S 2018 *International Journal of Heat and Mass Transfer* **127** 92
- [14] Albernaz D L, Amberg G and Do-Quang M 2016 *International Journal of Heat and Mass Transfer* **97** 853
- [15] Attia A M A and Kulchitskiy A R 2014 *Fuel* **116** 703
- [16] Shinjo J, Xia J, Ganippa L C and Megaritis A 2014 *Phys Fluids* **26**(10) 103302
- [17] Shinjo J, Xia J, Megaritis A, Ganippa L C and Cracknell R F 2016 *Atomization and Sprays* **26** 551
- [18] Shinjo J and Xia J 2017 *Proceedings of the Combustion Institute* **36** 2513

- [19] Sazhin S S, Rybdylova O, Crua C, Heikal M, Ismael M A, Nissar Z and Aziz A R B A 2019 *International J of Heat and Mass Transfer* **131** 815
- [20] Girin O G 2017 *Atomization and Sprays* **27** 407
- [21] Zhang Y, Huang Y, Huang R, Huang S, Ma Y, Xu S and Wang Z 2018 *Applied Thermal Engineering* **133** 633
- [22] Sazhin S S, Shchepakina E and Sobolev V 2018 *Combustion and Flame* **187** 122
- [23] Sazhin S S, Shchepakina E and Sobolev V 2019 *Journal of Engineering Mathematics* **114(1)** 1
- [24] Shchepakina E, Sobolev V A and Mortell M P 2014 *Singular Perturbations: Introduction to System Order Reduction Methods with Applications Springer Lecture Notes in Mathematics* **2114**

### Acknowledgments

S. Sazhin was supported by the EPSRC, UK (grant EP/M002608/1). V. Sobolev and E. Shchepakina were supported by the Ministry of Education and Science of the Russian Federation as part of a program of increasing the competitiveness of SSAU in the period 2013-2020.